

Intelligent Control and Systems

DOI: <https://doi.org/10.15407/kvt200.02.041>

UDC 519.688

GRITSHENKO V.I., Corresponding Member of NAS of Ukraine,
Director of International Research and Training
Center for Information Technologies and Systems
of the National Academy of Sciences of Ukraine
and Ministry of Education and Science of Ukraine
e-mail: vig@irtc.org.ua

VOLKOV O.Ye.,
Senior Researcher of the Intelligent Control Department
e-mail: alexvolk@ukr.net

BOGACHUK Yu.P., Ph.D. (Engineering),
Leading Researcher of the Intelligent Control Department
e-mail: dep185@irtc.org.ua

GOSPODARCHUK O.Yu.,
Senior Researcher of the Intelligent Control Department
e-mail: dep185@irtc.org.ua

KOMAR M.M.,
Researcher of the Intelligent Control Department
e-mail: nickkomar08@gmail.com

SHEPETUKHA Yu.M., Ph.D. (Engineering),
Leading Researcher of the Intelligent Control Department
e-mail: dep185@irtc.org.ua

VOLOSHENIUK D.O.,
Researcher of the Intelligent Control Department
e-mail: p-h-o-e-n-i-x@ukr.net
International Research and Training Center for Information
Technologies and Systems of the National Academy of Sciences
of Ukraine and of Ministry of Education and Science of Ukraine,
40, Acad. Glushkov av., Kyiv, 03187, Ukraine

INTELLECTUAL CONTROL, LOCALIZATION AND MAPPING IN GEOGRAPHIC INFORMATION SYSTEMS BASED ON ANALYSIS OF VISUAL DATA

Introduction. Nowadays, geoinformation systems (GIS) are widely used in transport, construction, navigation, geology, geography, military affairs, topography, economics and more.

Problem Statement. Modern GIS publications highlight a number of pressing issues regarding the need to develop technologies and methods for the rapid formation of spatial-temporal geoinformation data bases and dynamic mapping images. The process of prompt formation of cartographic images of the area of unmanned aerial vehicles (UAV) flights in GIS databases is based on the simultaneous solution of two problems — determining the location of UAV in space, as well as the formation of a mapping image of the area under study.

The purpose of the paper is to describe the method of topographic clustering of the obtained photographic images of UAV flights, which allows to combine visual images due to

the semantic search of their topographic similarity, in order to realize the visual localization of UAV and high-precision layout of the mapping image of the navigation environment in the operational GIS database.

Materials and methods. *The research conducted is based on the technologies of intelligent processing of large arrays of video and photo data, the theory of automatic control, methods of image processing and recognition based on descriptors of special points, methods of computer vision, as well as on methods and algorithms of own development, theory of navigation and dynamics of UAV flight.*

Results. *Procedures of topographic clustering of visual images obtained with UAV are developed, which are used for cognitive detection, description and matching among the characteristic features of the navigation environment.*

Conclusions. *The formation of a mapping image of the area of the navigation environment using the proposed method of topographic clustering of visual images achieved a decimeter accuracy in spatial coordinates, allowing visual localization and mapping with a high level of accuracy.*

Keywords: *unmanned aerial vehicle, geoinformation system, information technology, computer vision, intelligent control, cartographic image, aerial photography.*

INTRODUCTION

Nowadays geographic information systems (GIS) are widely used at such domains as transport, building, navigation, geology, geography, soldiery, topography, economy etc. However, modern publications about GIS indicate an amount of unsolved problems related to the necessity of space-time databases and dynamical mapping patterns operative formation technologies and methods development. Such data is necessary for fast reaction support of intellectual control systems that need to work in the real time scale under complex conditions of technological disasters, fire accidents, military operations, electronic or cyberattacks etc [1, 2].

The photographic aerial survey, provided by unmanned aerial vehicles is the most economically justified and effective remote way to supply the necessary and current information to GIS [3]. The operative formation process of the mapping patterns of the unmanned aerial vehicles (UAV) flying zones is based on the simultaneous solving of two problems — the UAV intellectual control that lies in definition of UAV location in space and also in corresponding area mapping pattern formation.

Today, the satellite systems as, for example, global positioning system are most commonly used for the global coordinates definition during the missions of UAV localization. But, due to various reasons, signals from navigation satellites can be unavailable, lost or functioning under “Spoofing attack” effect.

For this very reason the actual development direction is the support of reliable functioning of the UAV in full-autonomy mode, in other words without any signal of global positioning system. One of the modern ways of high-level autonomy achievement is simultaneous localization and mapping on the basis of just visual data usage problems solving [4, 5, 6]. In similar cases UAV visual localization accomplishes on the basis of computer vision methods and algorithms by the way of analysis and comparison of visual pictures special points, that were done by the UAV onboard camera [7, 8, 9]. The mission of simultaneous localization and mapping is building of the map in unknown space or map update in previously known space or with simultaneous intellectual control of the UAV and current location and passed route control. Complex

incorporation of the intellectual control theory, intellectual processing of video- and photo- data memory arrays technology, computer vision methods promotes expansion of geographic information system function capabilities by the production and purposeful usage of the environmental knowledge, creation of artificial intelligence elements and intellectualization of control processes.

The disadvantage of current visual data processing methods is that some of made decisions about special points matching cannot fit the real situation. It, foremost, can be caused by the specifics of pictures that are using for visual navigation, concretely by the big amount of small objects with low detailing. Availability of wrong fits of special points decreases accuracy of the visual navigation systems significantly and it can cause essential errors during the calculation of UAV visual coordinates and, under unfavorable conditions, leads to visual localization systems breakdown in general.

For the purpose of elimination of aforementioned disadvantages and limits of known computer vision methods, the methodology, algorithms and visual pictures topographic clustering procedures were developed. Usage of the information, received by the onboard UAV sensors for topographical clustering allows accomplishing the detection, description and reliable matching amongst characteristic features of the navigation environment. On this basement the intellectual component of UAV visual localization and highly accurate configuration of navigation environment mapping pattern are realized [10].

The formation of several UAV fly photographic patterns with usage of explored district surface air photos, that were made during such flies accomplishes for the construction of navigational space operation mapping (for example, fly 1 and fly 2 on Fig. 1).

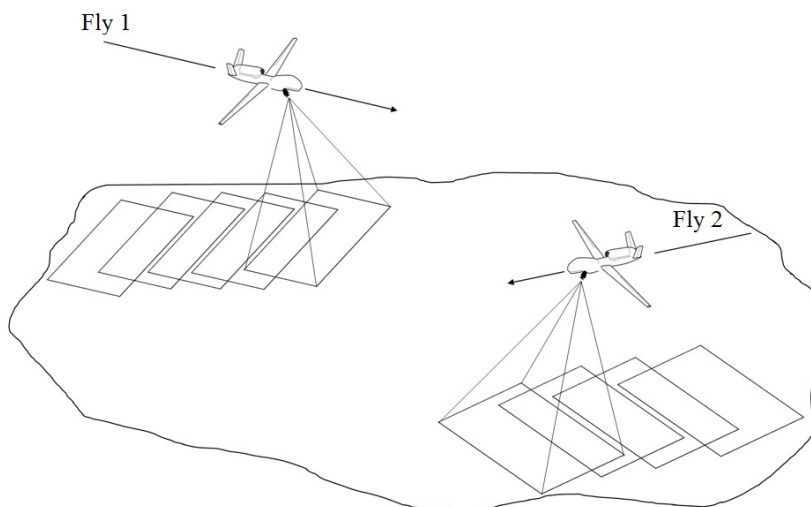


Fig. 1. Fly photographic pattern formation

The purpose of the paper is the development of the topographic clustering method for fly photographic patterns analysis received during the intellectual UAV control. Firstly, such analysis gives the possibility to accomplish UAV visual localization and secondly, allows accurate combining of visual images for construction of fly mapping pattern because of topographic similarities semantic search between images.

METHOD OF TOPOGRAPHIC CLUSTERING OF THE SEQUENCE OF VISUAL IMAGES, RECEIVED BY THE UNMANNED AERIAL VEHICLES

The vast majority of known visual image analysis methods are using detectors and descriptors, that detect specific points that are comparing with each other afterwards in the aim of formation of, so called, “matching point set”, other words identical points on different visual images. The biggest disadvantage of known visual image comparison methods is the fact that some amount of specific point’s matches can be incorrect [7, 8, 9]. One of the reasons of it is that even during the use of totally operable global satellite navigational system, mapping pattern formation sufficient accuracy is not guaranteed because of low accuracy rates of contemporary civil satellite navigation systems. Any error during the mapping pattern creation causes accuracy decreasing of the received map, and in some cases, full unsuitability of such map.

For the correction of such disadvantage the visual image topography clustering method is proposed. There are such features of this method as, firstly, the extraction to cluster from the established set of specific points accomplishes just for points that have some prescribed topographic features that are significantly differ such cluster points from other specific points of the established set. Another feature of the proposed method is that it has capability to check additionally (on the basis of visual image topographic features analysis) match point sets that has been received by known methods for the veracity. Matching points for visual images that have not pass the required check are interpreted as wrong and are excluded from the match point set that increases quality and reliability of visual image analysis significantly.

Furthermore, for the aim of much more detailed exposition of the visual image topographic clustering basic features method, it structures in the range of sequential procedures, each of that is an indispensable part for this method functional capabilities realization.

THE PROCEDURE OF SPECIFIC POINTS INDEXED ARRAYS FORMATION

The first of aforementioned procedures is a specific points indexed arrays formation procedure. Input data of this procedure is an organized set of three-element suites. Suites are formed as a result of sequential appliance of specific point extraction algorithms and their juxtaposition algorithms. Each suite consists of the following elements:

- specific point on the standard frame (hereafter — «default specific point»);
- specific point on the current frame (hereafter — «current specific point»);
- D numeric parameter that describes proximity degree (similitude degree) of suite specific points (hereafter — “distance”).

The similitude degree has been chosen in such a way that for absolutely identical points $D = 0$.

The set of the input data of the procedure could be presented in the following way:

$$\langle kp_i^b, kp_i^c, D_i \rangle, i = 1, 2, \dots, Q, \quad (1)$$

where kp_i^b, kp_i^c — i -th specific point on the standard and current image (other words b and c indexes are respectively indicate the affiliation of the specific point to the default and current image); Q — general quantity of specific points that are defined by the standard algorithm of basic points extraction.

The method uses the suites set sortation procedure (1) due to the increasing of distance D and chooses N first suites afterwards. Other words, the most approximate (alike) specific points of the default and current image are choosing.

Chosen suites number in the random order from 1 to N :

$$\left[\langle kp_i^b, kp_i^c, D_i \rangle \right], i = 1, 2, \dots, N. \quad (2)$$

Furthermore, due to the chosen suites, two indexed arrays are developed — the array of basic specific points (hereafter, the *BKP* array) and array of current specific points (hereafter, the *CKP* array). In the *BKP* array all basic specific points from the suites (2) are coming. In the *CKP* array all current specific points from suites (2) are coming. Herewith, both arrays are organized (indexed) with respect to numerical order (indexes) of suites that has been chosen by the formula (2):

$$\begin{aligned} BKP &= [kp_i^b] \\ CKP &= [kp_i^c] \end{aligned} \quad i = 1, 2, \dots, N \quad (3)$$

THE PROCEDURE OF BEARING THREE-POINT CLUSTERS EXTRACTION

The second by the sequence is the procedure of bearing three-point clusters extraction. For the procedure accomplishment, all possible three-points of the *BKP* array are enumerated (for such operation order of point processing in the triplet is insignificant). On the foremost step of the enumeration triplet of points is choosing:

$$(kp_i^b, kp_j^b, kp_k^b), \quad (4)$$

where $i = 1, \dots, N; j = i+1, \dots, N; k = j+1, \dots, N$.

Triplet of points from the *BKP* array can be considered as three-point cluster (hereafter, default three-point cluster). In the geometrical interpretation, three-point cluster surely defines some geometrical figure that can be named as “three-pointed cluster star”. The center of star (cluster mass center) can be named point, each coordinate of that is an arithmetical average value of corresponding point coordinates that are defined cluster. The rays of cluster star could be named vectors that are passing out from the star center to the each cluster specific point.

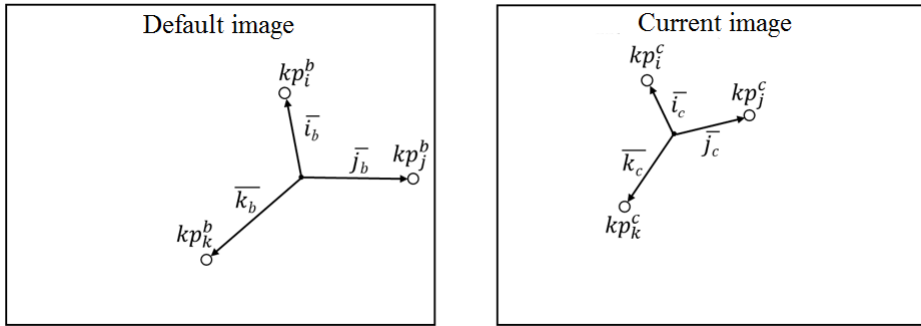


Fig. 2. Three-point cluster and its components for the default and current image

From the *CKP* array, the triplet of points chooses with indexes corresponding to the point indexes that are in cluster (4). Chosen point triplet creates current three-point cluster.

Cluster from the specific points of current image can be written in the following way:

$$(kp_i^c, kp_j^c, kp_k^c), \tag{5}$$

where $i = 1, \dots, N; j = i+1, \dots, N; k = j+1, \dots, N$.

Clusters (4) and (5) are creating pair that is depicted on the fig.2, for such pair the proximity (similarity) estimation procedure accomplishes later on.

THE PROCEDURE OF STANDARD AND CURRENT THREE-POINT CLUSTERS SIMILARITY EVALUATION

On this stage the method works in cycle, where in the first iteration the pair of *i*-th ray is considered as bearing. After that the *LR* scale coefficient is calculated as a correlation of the default cluster bearing ray length $|\bar{i}_b|$ to the current cluster ray length $|\bar{i}_c|$:

$$LR = \frac{|\bar{i}_b|}{|\bar{i}_c|}. \tag{6}$$

Afterwards the method calculates the ray azimuth difference between default and current cluster (Az_{diff}) by the formula:

$$Az_{diff} = Az(\bar{i}_b) - Az(\bar{i}_c), \tag{7}$$

where $Az(\bar{i}_b)$ — *i*-th ray azimuth of the default cluster; $Az(\bar{i}_c)$ — *i*-th ray azimuth of the current cluster.

The star rays are scaling including the *LR* (6) scale coefficient. After it cluster stars of the default and current image are united in the way that cluster star centers and bearing rays are coinciding. Herewith, current cluster star turning on the angle Az_{diff} (7) also takes place:

$$\begin{aligned}\bar{i}_{c_{sr}} &= M(Az_{diff}) \cdot (\bar{i}_c \cdot LR); \\ \bar{j}_{c_{sr}} &= M(Az_{diff}) \cdot (\bar{j}_c \cdot LR); \\ \bar{k}_{c_{sr}} &= M(Az_{diff}) \cdot (\bar{k}_c \cdot LR),\end{aligned}\tag{8}$$

where $\bar{i}_{c_{sr}}$, $\bar{j}_{c_{sr}}$, $\bar{k}_{c_{sr}}$ — rays of the scaled and turned current cluster star; M — turning matrix on the angle Az_{diff} .

For each of the rays the error range Er is defined, that is scaled to the dimensionless form with the invariance assurance to the cluster scale:

$$\begin{aligned}Er_{ij} &= \frac{|\bar{j}_b - \bar{j}_{c_{sr}}|}{|\bar{j}_b|}; \\ Er_{ik} &= \frac{|\bar{k}_b - \bar{k}_{c_{sr}}|}{|\bar{k}_b|}.\end{aligned}\tag{9}$$

If the error range Er of, at least, one pair of rays appears to be greater than prescribed limit value, the closeness (similarity) estimation of such default and current three-point clusters finishes with failure and the procedure returns to the stage of extraction of another one three-point cluster.

If Er error ranges for each ray pair turn to be less then prescribed limit level, method calculates the cluster similarity error CER for chosen pair of bearing rays by the formula:

$$CER_{ijk} = Er_{ij} + Er_{ik}.\tag{10}$$

In the second iteration, vector \bar{j} is chosen as a bearing vector and the above-described procedure by the formulas (6)–(10) takes place again.

LR scale coefficient calculates by the formula:

$$LR = \frac{|\bar{j}_b|}{|\bar{j}_c|}.\tag{11}$$

Default and current cluster ray azimuth difference (Az_{diff}) equals to:

$$Az_{diff} = Az(\bar{j}_b) - Az(\bar{j}_c).\tag{12}$$

Scaled and turned rays of the current cluster star can be found by the formula (8). For each of the rays error range Er can be calculated by the formula:

$$Er_{ji} = \frac{|\bar{i}_b - \bar{i}_{c_{sr}}|}{|\bar{i}_b|};$$

$$Er_{jk} = \frac{|\bar{k}_b - \bar{k}_{c_{sr}}|}{|\bar{k}_b|}.$$
(13)

Afterwards, the condition of error limit value non-overrunning is checking.

After, the error of cluster similarity CER for chosen pair of bearing rays is calculating by the formula:

$$CER_{jik} = Er_{ji} + Er_{jk}.$$
(14)

In the third iteration, the method chooses vector \bar{k} as a bearing vector. Scaled LR coefficient can be found by the formula:

$$LR = \frac{|\bar{k}_b|}{|\bar{k}_c|}.$$
(15)

Default and current cluster rays azimuth difference (Az_{diff}) is equal to:

$$Az_{diff} = Az(\bar{k}_b) - Az(\bar{k}_c).$$
(16)

Scaled and turned rays of the current cluster star can be found by the formula (8).

For each of the rays error range Er can be calculated by the formula:

$$Er_{ki} = \frac{|\bar{i}_b - \bar{i}_{c_{sr}}|}{|\bar{i}_b|};$$

$$Er_{kj} = \frac{|\bar{j}_b - \bar{j}_{c_{sr}}|}{|\bar{j}_b|}.$$
(17)

Afterwards, the condition of error limit value non-overrunning is checking.

After, the error of cluster similarity CER for chosen pair of bearing rays is calculating by the formula:

$$CER_{kij} = Er_{ki} + Er_{kj}.$$
(18)

As a closeness (similarity) error CE of the default and current three-point clusters, the minimal value between CER_{ijk} , CER_{jik} , CER_{kij} chooses:

$$CE^{ijk} = \min(CER_{ijk}, CER_{jik}, CER_{kij}).$$
(19)

After that, the procedure returns to the selection of a new point triplet in enumeration cycle of all possible point triplets from the BKP array.

After the finish of enumeration of all possible triplets as bearing three-point clusters, a pair (default and current three-point cluster) is choosing, for which the CE value is minimal. If CE calculation has failed for each pair of three-point clusters, it

shall be deemed that bearing cluster extraction procedure on the default and current images on the basis of the specific points comparison results has failed.

Default bearing cluster is written in the following way:

$$(kp_{i_o}^b, kp_{j_o}^b, kp_{k_o}^b). \quad (20)$$

Current bearing cluster is written in the following way:

$$(kp_{i_o}^c, kp_{j_o}^c, kp_{k_o}^c). \quad (21)$$

THE PROCEDURE OF SUPPLEMENTAL POINT ADDITION INTO THE BEARING STANDARD THREE-POINT CLUSTERS

During the accomplishment of this procedure, each point of the *BKP* array that has not been included to the bearing default three-point cluster are enumerating cyclically.

Chosen point $kp_l^b, l = 1, \dots, N; l \neq i_o; l \neq j_o; l \neq k_o$, from the *BKP* array adds to the bearing default three-point cluster and creates default four-point cluster.

From the *CKP* array the kp_l^c point is choosing that forms a pair with kp_l^b from the *BKP* array. Chosen point from the *CKP* array adds to the bearing current three-point cluster and forms current four-point cluster (Fig. 3).

4th-point cluster default cluster can be written in the following way:

$$(kp_{i_o}^b, kp_{j_o}^b, kp_{k_o}^b, kp_l^b). \quad (22)$$

4th-point cluster current cluster can be written in the following way:

$$(kp_{i_o}^c, kp_{j_o}^c, kp_{k_o}^c, kp_l^c). \quad (23)$$

In the geometric interpretation each of four-point clusters (22) and (23) defines unambiguously some geometrical figure that can be named “four-rayed cluster star”. The point, each coordinate of that is an arithmetic average value of the corresponding cluster-forming point coordinates can be named the star center (the mass center). As star rays can be named vectors that are tracing from the star center to each cluster-forming point.

On the first iteration the method considers i -th rays pair $(\bar{i}_o^b, \bar{i}_o^c)$ as bearing.

The next step of the method calculates *LR* scale coefficient as correlation of the default cluster bearing ray length \bar{i}_o^b to the current cluster bearing ray length \bar{i}_o^c :

$$LR = \frac{|\bar{i}_o^b|}{|\bar{i}_o^c|}. \quad (24)$$

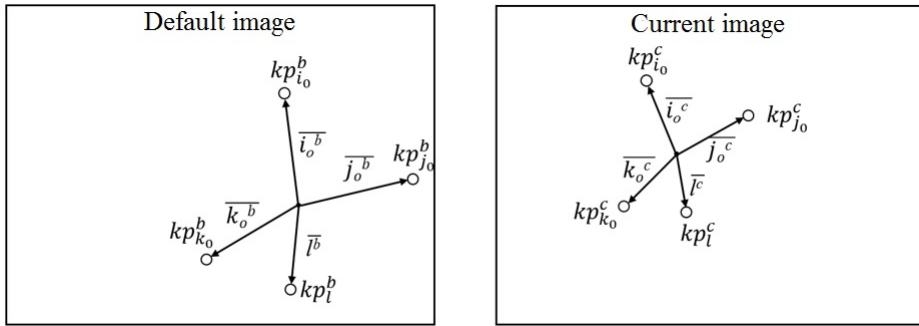


Fig. 3. Additional point adjunction in the bearing three-point clusters

Afterwards the method calculates the difference between bearing ray azimuths of default and current clusters of (Az_{diff}) by the formula:

$$Az_{diff} = Az(\bar{i}_o^b) - Az(\bar{i}_o^c), \quad (25)$$

where $Az(\bar{i}_o^b)$ — i -th azimuth of the default cluster bearing ray; $Az(\bar{i}_o^c)$ — i -th azimuth of the current cluster bearing ray.

The current cluster star rays are scaling including LR scale coefficient. After it cluster stars of the default and current clusters are united in such a way that cluster star centers and bearing rays are coinciding. Herewith, current cluster star turning on the angle Az_{diff} also takes place:

$$\begin{aligned} \bar{i}_{o_{sr}}^c &= M(Az_{diff}) \cdot (\bar{i}_o^c \cdot LR); \\ \bar{j}_{o_{sr}}^c &= M(Az_{diff}) \cdot (\bar{j}_o^c \cdot LR); \\ \bar{k}_{o_{sr}}^c &= M(Az_{diff}) \cdot (\bar{k}_o^c \cdot LR); \\ \bar{l}_{sr}^c &= M(Az_{diff}) \cdot (\bar{l}^c \cdot LR), \end{aligned} \quad (26)$$

where $\bar{i}_{o_{sr}}^c$, $\bar{j}_{o_{sr}}^c$, $\bar{k}_{o_{sr}}^c$, \bar{l}_{sr}^c — rays of the scaled and turned current cluster star; M — turning matrix on the angle Az_{diff} .

The Er error range for pair of default and current rays of the additional point kp_l (\bar{l}^b and \bar{l}_{sr}^c) defines:

$$Er_{il} = \frac{|\bar{l}^b - \bar{l}_{sr}^c|}{|\bar{l}^b|}. \quad (27)$$

If Er appears to be greater than prescribed limit value, current pair of specific points excludes from the list of candidates for including to default and current clusters, the procedure passes to the step of a new candidate points pair choosing for the including to the cluster.

On the next two iterations, remained ray pairs of three-rayed default and current clusters are considering as bearing. For the situation, depicted on the fig. 3 — there are ray pairs $(\bar{j}_o^c, \bar{j}_o^b)$ and $(\bar{k}_o^c, \bar{k}_o^b)$. After it, each action that has been described by formulas (24) – (27) repeats for a new chosen pair of bearing rays.

If after the finish of the cycle the error range has not overpass prescribed limit value than current pair of points (kp_i^c, kp_i^b) for fig. 3) marks as a candidate for including to the default and current clusters respectively, after that procedure passes to the step of another point-candidate choosing for including in cluster.

After the ending of candidate points cyclical enumeration for the including in cluster, all default and bearing points, marked as candidates for including in default and current clusters (fulfilled condition about limit value overpassing absence) are adding to the corresponding cluster. As a result, there is a cluster pair — default and current S-point clusters, where $S \geq 3$ and $S \leq N$.

Other words, S-point cluster consists of bearing three-point cluster with adding of all points, for which the condition of the limit value overpassing absence is fulfilled.

SIMILAR CLUSTERS EMPHASIS BY THE SPECIFIC POINT COMPARISON RESULTS THAT HAVE BEEN RECEIVED BY THE ALTERNATIVE METHOD OF SPECIFIC POINTS EMPHASIS

Each procedure of method work (1–27), described in 2.2–2.4 repeats for sets of three-element tuples that are constructed by another (alternative) specific point extracting method (during the usage of OpenCV library [11], for this aim algorithms BRISK, ORB, AKAZE can be used). If the primary (by the first method) and repetitive (by the second method) procedure of similar cluster extraction procedure fails, it is regarded that clusterization procedure failed for given image pair. Clusterization procedure for given image pair ends.

If similar cluster extraction procedure has ended successfully, there are two pairs of similar clusters: the S S-point cluster pair for the first algorithm of specific point extraction and the S' S'-point cluster pair for the second (alternative) algorithm of specific point extraction. So that two pairs are the input data for the cluster cross-check procedure.

CLUSTER CROSS-CHECK PROCEDURE

The verification of similar cluster extraction results by the specific point comparison results proceeds by the cluster cross-check procedure that resides in expansion of the first received cluster by the second cluster points.

Herewith, the first cluster pair S is considered to be basic and the second one S' — additional. From the S cluster pair default and current three-point bearing clusters (20) and (21) are extracted.

After that each point pairs of the S' cluster extra pair are enumerating cyclically for its adding to the S cluster. Three-point default and current bearing clusters are furnished out by the corresponding specific point from another pair of cluster points S' and form four-point cluster pair: default and current four-point cluster (Fig. 4).

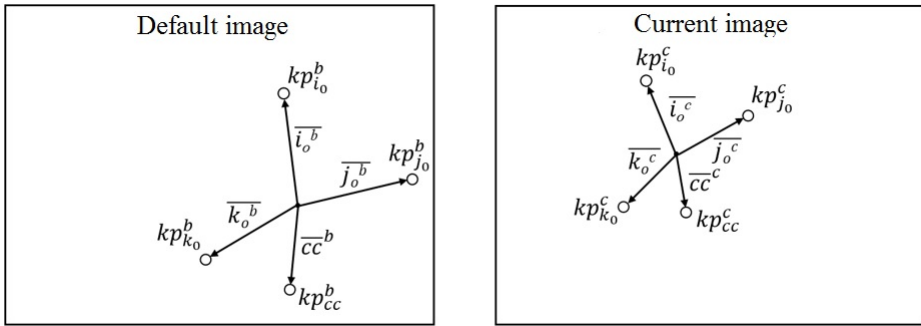


Fig. 4. Cross-check procedure

On Fig. 4: $(kp_{i_0}^b, kp_{j_0}^b, kp_{k_0}^b)$ — bearing default cluster of the S -point cluster for the first algorithm of specific point extraction; $(kp_{i_0}^c, kp_{j_0}^c, kp_{k_0}^c)$ — bearing current cluster of the S -point cluster for the first specific point extraction algorithm; kp_{cc}^b, kp_{cc}^c — point-candidate pair for the expansion of S clusters from the extra S' clusters.

Further work of the method is similar to the procedure of extra point addition to the bearing clusters, described in the 2.4 sub-paragraph.

4-point default cluster can be written in the following way:

$$(kp_{i_0}^b, kp_{j_0}^b, kp_{k_0}^b, kp_{cc}^b). \quad (28)$$

4-point current cluster can be written in the following way:

$$(kp_{i_0}^c, kp_{j_0}^c, kp_{k_0}^c, kp_{cc}^c). \quad (29)$$

Each of four-point clusters (28) and (29) defines the four-ray star unambiguously. The cluster mass center is the center of the star. Rays of the star are vectors that begin at the star center and direct to the each point that forms cluster.

The method considers pair of i -th rays $(\vec{i}_0^b, \vec{i}_0^c)$ as bearing on the first iteration.

The next step of the method calculates LR scale coefficient as correlation between default cluster bearing ray length \vec{i}_0^b and current cluster bearing ray length \vec{i}_0^c by the formula (24).

Afterwards method calculates the difference between ray azimuths of default and current clusters (Az_{diff}) by the formula (25).

Current cluster star rays are scaling including LR scale coefficient. After that current and default image cluster stars are united in such a way that cluster star centers and bearing rays are coinciding. Herewith, current cluster star turning on the angle Az_{diff} also takes place:

$$\begin{aligned}
 \bar{i}_{o_{sr}}^c &= M(Az_{\text{diff}}) \cdot (\bar{i}_o^c \cdot LR); \\
 \bar{j}_{o_{sr}}^c &= M(Az_{\text{diff}}) \cdot (\bar{j}_o^c \cdot LR); \\
 \bar{k}_{o_{sr}}^c &= M(Az_{\text{diff}}) \cdot (\bar{k}_o^c \cdot LR); \\
 \bar{cc}_{sr}^c &= M(Az_{\text{diff}}) \cdot (\bar{cc}^c \cdot LR),
 \end{aligned} \tag{30}$$

where $\bar{i}_{o_{sr}}^c$, $\bar{j}_{o_{sr}}^c$, $\bar{k}_{o_{sr}}^c$, \bar{cc}_{sr}^c — scaled and turned current cluster star rays; M — turning matrix on the angle Az_{diff} .

The error range Er calculates for the pair of default and current rays of the extra point kp_{cc} (\bar{cc}^b and \bar{cc}_{sr}^c):

$$Er_{icc} = \frac{|\bar{cc}^b - \bar{cc}_{sr}^c|}{|\bar{cc}^b|}. \tag{31}$$

If Er turns to be greater than prescribed limit level, current pair of specific points excludes from the candidates on including in default and current clusters, method passes to the step of another candidate-point pair choosing from additional clusters.

On the next two iterations, remained ray pairs of three-rayed default and current clusters are considering as bearing. For the situation, depicted on fig. 4 – there are ray pairs $(\bar{j}_o^c, \bar{j}_o^b)$ and $(\bar{k}_o^c, \bar{k}_o^b)$. Afterwards the algorithm repeats each action that has been described in formulas (24, 25, 30, 31) for the new pair of chosen bearing rays.

If after the cycle ending the error range Er does not overrun prescribed limit value than current point pair (kp_{cc}^b, kp_{cc}^c) for fig. 4) marks as candidate for expansion of the basic default and current clusters respectively, after that method passes to another pair of points selection from the additional cluster pair S' .

After the finish of cyclic point enumeration from the additional cluster pair S' , each additional cluster point pairs marked as candidates for including in the basic cluster pair are adding to basic default and current cluster S . So another cluster pair is forming: extended default cluster and extended current cluster S_{extended} .

After full cross-check procedure accomplishes repeatedly, only for the case, when S' cluster pair is basic and S cluster pair is additional.

After the finish of cyclic point enumeration with the additional cluster pair S , all additional cluster point pairs that marked as candidates for including in the basic cluster pair are adding to basic default and current cluster S' . So the cluster pair is forming: extended basic cluster and extended current cluster S'_{extended} .

Clusterization procedure summarizing results are forming in the following way:

- if during the cross-check extension of S cluster pair has failed by the two point pairs from the additional cluster pair S' minimally and also failed to extend S' cluster pair by two point pairs from the additional cluster pair S , its deemed that clusterization procedure has failed for the given pair of images.

– on the other case, cluster pair ($S_{extended}$ or $S'_{extended}$) to what greater number of points from additional cluster has been added chooses as a resulting cluster pair. If the number of added point pairs in $S_{extended}$ and $S'_{extended}$ clusters is equal, the first pair is selected as the result.

Two points comparison reliability is achieving due to the fact that visual image matching points that have not passed visual image topographic feature check are interpreting as false and excluding from the matching point set.

The developed visual image topographic clusterization method utilization offers an opportunity to reduce the possibility of false match appearing significantly. Results of conducted experiments based on the real flight data showed that utilization of search, description and comparison of specific points methods including the visual image topographic clusterization method provides the significant reduce of the false match appearing possibility during the image comparison that is utilizing in intellectual control systems for highly-accurate UAV autonomous navigation support.

CONCLUSIONS

Developed visual image topographic clusterization procedures provided by the UAV are applicable to the computer vision methods that are applying to cognitive definition, description and matching determination amongst the navigation environment characteristic features and realizing intellectual part of the informational technology that could be successfully implemented to the UAV control system for the autonomy coordinate location and forming of the flight geoinformation patterns in GIS information databases.

Mentioned modelling and real flight testing results showed that exploring topographic environment area mapping pattern including the usage of the proposed visual image topographic clusterization method achieving the decimeter accurateness for space coordinates that gives a possibility to accomplish visual localization and mapping with the high level accurateness. Availability of such data level accurateness simplifies processing significantly and allows accomplishing processing stages in full-automatic mode.

According to authors, the perspective way is to continue experiments at the domain of full switching to the autonomous navigation for UAV coordinate determination mission during the simultaneous solving of the localization and mapping problems. Proposed method would expand the variety of the UAV usage by increasing of the UAV intellect and autonomy level that would have positive influence on the active manufacturing rising and on the increasing of the UAV complexes usage in Ukraine and all over the world.

Also, suggested method can be implemented in the perspective intellectual control systems that are demanding modelling of conscious behavior of the human, who extracts the data, that is necessary for environment features perception.

REFERENCES

1. Artes T., Cencerrado A., Cortes A., Margalef T. Real-time genetic spatial optimization to improve forest fire spread forecasting in high-performance computing environments. *International Journal of Geographical Information Science*. 2016, Vol. 30, № 3, pp. 594–611.
2. Li J., Bi Y., Lan M., Qin H., Shan M., Lin F., Chen B.M. Real-time Simultaneous Localization and Mapping for UAV: A Survey. *Proc. of International micro air vehicle competition and conference*. 2016, Beijing, China, 2016, pp. 237–242.

3. Kozub, A. M., Suvorova, N. O., & Chernyavsky, V. M. Analiz zasobiv zboru informatsiyi dlya heorafichnykh informatsyinykh system. *Systemy ozbroynnya i viyskova tekhnika*. 2011, №3, pp. 42–47. (In Ukrainian)
4. Gonzales D., Harting S. Designing Unmanned Systems with Greater Autonomy: Using a Federated, Partially Open Systems Architecture Approach. Santa Monica, Calif: RAND, 2014, 96 p.
5. Agunbiade O., Zuva T., A Review: Simultaneous Localization and Mapping in Application to Autonomous Robot. *Preprints 2018*. 2018050293 (doi: 10.20944/preprints201805.0293.v1).
6. Fuentes-Pacheco J., Ruiz-Ascencio J., Rendon-Mancha J.M. Visual simultaneous localization and mapping: a survey. *Artificial Intelligence Review*. 2015, Vol. 43, №1, pp. 55–81.
7. Silpa C., Hartley R. Optimised KD-trees for fast image descriptor matching. *Proceedings of the IEEE Conference on Computer Vision and Pattern Recognition*. 2008, pp. 1–8.
8. Dufournaud Y., Schmid C., Horaud R. Image matching with scale adjustment. *Computer Vision Image Understanding*. 2004, № 93(2), pp. 175–194.
9. Zhang W., Kosecka J. Image based localization in urban environments. *Proceedings of the Third International Symposium on 3D Data Processing, Visualization, and Transmission*. 2006, Chapel Hill, USA, pp. 33–40.
10. Schubert J., Brynielsson J., Nilsson M., Svenmarck P. Artificial Intelligence for Decision Support in Command and Control Systems. *Proceedings of the 23rd International Command and Control Research & Technology Symposium «Multi-Domain C2»*. 2018, Playa Vista, California, USA, pp. 18–33.
11. Bradski G., Kaehler A. Learning OpenCV. O'Reilly Media, 2008, 576 p.

Received 27.02.2020

ЛІТЕРАТУРА

1. Artes T., Cencerrado A., Cortes A., Margalef T. Real-time genetic spatial optimization to improve forest fire spread forecasting in high-performance computing environments. *International Journal of Geographical Information Science*. 2016. Vol. 30, № 3. P. 594–611.
2. Li J., Bi Y., Lan M., Qin H., Shan M., Lin F., Chen B.M. Real-time Simultaneous Localization and Mapping for UAV: A Survey. *Proc. of International micro air vehicle competition and conference*. 2016. Beijing, China, 2016. P. 237–242.
3. Козуб А.М., Суворова Н.О., Чернявський В.М. Аналіз засобів збору інформації для географічних інформаційних систем. *Системи озброєння і військова техніка*. 2011. № 3. С. 42–47.
4. Gonzales D., Harting S. Designing Unmanned Systems with Greater Autonomy: Using a Federated, Partially Open Systems Architecture Approach. Santa Monica, Calif: RAND. 2014. 96 p.
5. Agunbiade O., Zuva T., A Review: Simultaneous Localization and Mapping in Application to Autonomous Robot. *Preprints 2018*. 2018050293 (doi: 10.20944/preprints201805.0293.v1).
6. Fuentes-Pacheco J., Ruiz-Ascencio J., Rendon-Mancha J.M. Visual simultaneous localization and mapping: a survey. *Artificial Intelligence Review*. 2015. Vol. 43. №1. P. 55–81.
7. Silpa C., Hartley R. Optimised KD-trees for fast image descriptor matching. *Proceedings of the IEEE Conference on Computer Vision and Pattern Recognition*. Alaska, 2008. P. 1–8.
8. Dufournaud Y., Schmid C., Horaud R. Image matching with scale adjustment. *Computer Vision Image Understanding*. 2004. № 93(2). P. 175–194.
9. Zhang W., Kosecka J. Image based localization in urban environments. *Proceedings of the Third International Symposium on 3D Data Processing, Visualization, and Transmission*. Chapel Hill, USA. 2006. P. 33–40.
10. Schubert J., Brynielsson J., Nilsson M., Svenmarck P. Artificial Intelligence for Decision Support in Command and Control Systems. *Proceedings of the 23rd International Command and Control Research & Technology Symposium «Multi-Domain C2»*. Playa Vista, California, USA. 2018. P. 18–33.
11. Bradski G., Kaehler A. Learning OpenCV. O'Reilly Media, 2008. 576 p.

Отримано 27.02.2020

Гриценко В.І., член-кореспондент НАН України,
директор Міжнародного науково-навчального центру
інформаційних технологій та систем
НАН України та МОН України
e-mail: vig@irtc.org.ua

Волков О.Є.,
старш. наук. співроб.
відд. інтелектуального управління
e-mail: alexvolk@ukr.net

Богачук Ю.П., канд. техн. наук,
пров. наук. співроб.
відд. інтелектуального управління
e-mail: dep185@irtc.org.ua

Господарчук О.Ю.,
старш. наук. співроб.
відд. інтелектуального управління
e-mail: dep185@irtc.org.ua

Комар М.М.,
наук. співроб.
відд. інтелектуального управління
e-mail: nickkomar08@gmail.com

Шенетуха Ю.М., канд. техн. наук,
пров. наук. співроб.
відд. інтелектуального управління
e-mail: dep185@irtc.org.ua

Волошенюк Д.О.,
наук. співроб.
відд. інтелектуального управління
e-mail: p-h-o-e-p-i-x@ukr.net

Міжнародний науково-навчальний центр інформаційних технологій
та систем НАН України та МОН України,
пр. Акад. Глушкова 40, м. Київ, 03187, Україна

ІНТЕЛЕКТУАЛЬНЕ КЕРУВАННЯ, ЛОКАЛІЗАЦІЯ ТА КАРТОГРАФУВАННЯ В ГЕОІНФОРМАЦІЙНИХ СИСТЕМАХ НА ОСНОВІ АНАЛІЗУ ВІЗУАЛЬНИХ ДАНИХ

Вступ. У сьогоденні геоінформаційні системи (ГІС) широко застосовують в транспорті, будівництві, навігації, геології, географії, військовій справі, топографії, економіці тощо.

Проблематика. Сучасні публікації у галузі ГІС висвітлюють ряд нагальних проблем щодо необхідності розроблення технологій та методів оперативного формування баз просторово-часових геоінформаційних даних та динамічних картографічних образів. Процес оперативного формування картографічних образів області польотів безпілотних літальних апаратів (БпЛА) в базах даних ГІС базується на одночасному розв'язанні двох завдань — визначенні місцезнаходження БпЛА у просторі, а також формуванні картографічного образу області, яка досліджується.

Мета. Опис методу топографічної кластеризації отриманих фотографічних образів польотів БпЛА, що дає змогу поєднувати візуальні зображення за рахунок семантичного пошуку їх топографічної подібності, з метою здійснення візуальної локалізації БпЛА та високоточної компоновки картографічного образу навігаційного середовища в оперативній базі даних ГІС у інтелектуальному керуванні.

Матеріали й методи. Проведені дослідження базуються на технології інтелектуального оброблення великих масивів відео- та фото-даних, теорії автоматичного керування, методів оброблення та розпізнавання зображень на основі дескрипторів особливих точок, методів комп'ютерного зору, а також на методах й алгоритмах власної розробки, теорії навігації та динаміки польоту БпЛА.

Результати. Розроблено процедури топографічної кластеризації візуальних зображень, отриманих за допомогою БпЛА, що застосовуються для когнітивного виявлення, опису і знаходження відповідності серед характерних ознак навігаційного середовища.

Висновки. Формування картографічного образу області навігаційного середовища з використанням запропонованого методу топографічної кластеризації візуальних зображень сягає дециметрової точності за просторовими координатами, що дає змогу виконувати візуальну локалізацію та картографування з високим рівнем точності.

Ключові слова: *Безпілотний літальний апарат, геоінформаційна система, інформаційні технології, комп'ютерний зір, інтелектуальне керування, картографічний образ, аерофотознімок*

Гриценко В.И., член-корреспондент НАН України,
директор Международного научно-учебного центра
информационных технологий и систем
НАН Украины и МОН Украины
e-mail: vig@irtc.org.ua

Волков А.Е.,
старш. науч. сотр.
отд. интеллектуального управления
e-mail: alexvolk@ukr.net

Богачук Ю.П., канд. техн. наук,
ведущ. науч. сотр.
отд. интеллектуального управления
e-mail: dep185@irtc.org.ua

Господарчук А.Ю.,
старш. науч. сотр.
отд. интеллектуального управления
e-mail: dep185@irtc.org.ua

Комар Н.Н.,
науч. сотр.
отд. интеллектуального управления
e-mail: nickkomar08@gmail.com

Шенетуха Ю.М., канд. техн. наук,
ведущ. науч. сотр.
отд. интеллектуального управления
e-mail: dep185@irtc.org.ua

Волошенко Д.А.,
науч. сотр.
отд. интеллектуального управления
e-mail: p-h-o-e-n-i-x@ukr.net

Международный научно-учебный центр информационных
технологий и систем НАН Украины и МОН Украины,
пр. Акад. Глушкова, 40, г. Киев, 03187, Украина

**ИНТЕЛЛЕКТУАЛЬНОЕ УПРАВЛЕНИЕ, ЛОКАЛИЗАЦИЯ
И КАРТОГРАФИРОВАНИЕ В ГЕОИНФОРМАЦИОННЫХ СИСТЕМАХ
НА ОСНОВЕ АНАЛИЗА ВИЗУАЛЬНЫХ ДАННЫХ**

Введение. В настоящее время геоинформационные системы (ГИС) широко применяются в транспорте, строительстве, навигации, геологии, географии, военном деле, топографии, экономике и т.д.

Проблематика. Современные публикации в области ГИС освещают ряд насущных проблем о необходимости разработки технологий и методов оперативного формирования

баз пространственно-временных геоинформационных данных и динамических картографических образов. Процесс оперативного формирования картографических образов области полетов беспилотных летательных аппаратов (БПЛА) в базах данных ГИС базируется на одновременном решении двух задач — определения местоположения БПЛА в пространстве, а также формирования картографического образа исследуемой области.

Цель. Описание метода топографической кластеризации полученных фотографических образов полетов БПЛА, что позволяет объединять визуальные изображения за счет семантического поиска их топографического сходства с целью осуществления визуальной локализации БПЛА и высокоточной компоновки картографического образа навигационной среды в оперативной базе данных ГИС при интеллектуальном управлении.

Материалы и методы. Проведенные исследования базируются на технологии интеллектуальной обработки больших массивов видео- и фото-данных, теории автоматического управления, методов обработки и распознавания изображений на основе дескрипторов особых точек, методов компьютерного зрения, а также на методах и алгоритмах собственной разработки, теории навигации и динамики полета БПЛА.

Результаты. Разработаны процедуры топографической кластеризации визуальных изображений, полученных с помощью БПЛА, применяемых для когнитивного выявления, описания и нахождения соответствия среди характерных признаков навигационной среды.

Выводы. Формирование картографического образа области навигационной среды с использованием предложенного метода топографической кластеризации визуальных изображений достигает дециметровой точности по пространственным координатам, что позволяет выполнять визуальную локализацию и картографирование с высокой степенью точности.

Ключевые слова: *Беспилотный летательный аппарат, геоинформационная система, информационные технологии, компьютерное зрение, интеллектуальное управление, картографический образ, аэрофотоснимок.*